Quaternary Research 79 (2013) 101–109

Contents lists available at SciVerse ScienceDirect

Quaternary Research

journal homepage: www.elsevier.com/locate/yqres

A lacustrine sedimentary record of Holocene periglacial activity from the Uinta Mountains, Utah, U.S.A.

Jeffrey S. Munroe *, Catherine M. Klem, Matthew F. Bigl

Geology Department, Middlebury College, Middlebury, VT 05753, USA

ARTICLE INFO

Article history:
Received 22 May 2012
Available online 24 January 2013

Keywords:
Holocene
Periglacial
Lacustrine sediment
Uinta Mountains
Utah

ABSTRACT

A lake sediment core from the Uinta Mountains of northern Utah was analyzed to constrain the timing of late Holocene periglacial activity. Records of numerous physical properties were converted to time series spanning the past 5300 years using a depth-age model based on four AMS ^{14}C dates. Long-term decreases in organic content and increases in bulk density attest to increasing inputs of clastic sediment. Abundance of mineral P, signaling physical bedrock weathering, reaches maximum values ca. 2900, 2150, and 1400 cal yr BP, coincident with finer median grain size and a shift toward darker red sediment. These peaks, interpreted as signals of periglacial activity, align with pulses of rock glacier activity in Colorado determined from lichenometry. The youngest peak coincides with lichenometric ages previously determined for periglacial deposits upstream from the lake. A pulse of renewed periglacial activity ca. 400 cal yr BP represents the Little Ice Age. The late 20th century witnessed extremely high values of organic matter and biogenic silica, and unprecedented low values of C:N, reflecting greatly enhanced in-lake productivity, likely due to disturbance in the watershed.

Introduction

Improved understanding of natural climate variability during the late Quaternary is an important goal of paleoclimate research and is crucial for evaluating evidence for anthropogenic climate change. Identification of climate forcing mechanisms operating over geologically recent time scales is also necessary for improving the predictive power of numerical climate models. Mountain regions, especially those featuring large amounts of ice near its melting point, are sensitive areas in which to evaluate evidence of past climate changes. Accordingly, numerous studies have focused on developing chronologies for fluctuations of alpine glaciers, both during the last glacial maximum (LGM) and the Holocene neoglaciation (e.g., Schaefer et al., 2006; Davis et al., 2009).

Paleoclimate information can also be extracted from periglacial landforms such as rock glaciers (Millar and Westfall, 2008), which is useful in regions where ice glaciers are absent. Rock glaciers are widely distributed in alpine environments where they occur as tongue-shaped or lobate deposits of rock and ice that move slowly downslope through internal deformation of ice (Wahrhaftig and Cox, 1959). They form where frequent freeze–thaw cycles enhance physical weathering of bedrock, and locally steep slopes facilitate accumulation of dislodged rock as talus. Ice-cored rock glaciers originate when talus overwhelms snowfall and ice flow rates, completely burying a preexisting ice glacier. Ice-cemented rock glaciers are produced when talus interstices become filled with ice, which subsequently deforms. These two features occupy opposite ends of a continuum of related landforms, all of which involve slow creep of rock and ice mixtures away from source areas (Clark et al., 1998).

The climatic relevance of rock glaciers hinges on the requirement of internal ice in sufficient volumes to deform and carry the landform forward. This ice is perennial, and as with other permafrost landforms, changes in the ground thermal regime resulting in a negative mass balance of ice may bring the rock glacier to a halt. However, unlike ice glaciers that may leave behind only scattered erratics and patches of till to mark their former presence, rock glaciers are preserved on the landscape after ice melt-out as conspicuous bulging lobes of rock debris, often featuring an oversteepened terminal slope and surface furrows testifying to the former motion of the now fossil landform (Wahrhaftig and Cox, 1959).

It is this combination of climatic dependence, high preservation potential, and diagnostic geomorphology that makes rock glaciers useful for alpine paleoclimate research. Unfortunately, because they are fundamentally unconsolidated piles of angular rock fragments, it has proven difficult to date rock glaciers directly. Indirect methods, including lichenometry and relative weathering criteria, have instead generated the most significant chronologies of past rock glacier activity (e.g., Benedict, 1967; Nicholas and Butler, 1996). Another option, common for studies of past glacier behavior but less often applied in periglacial settings, is the analysis of sediment records from lakes hydrologically connected to rock glaciers (e.g., Zielinski, 1989; Paasche et al., 2007). Clast-to-clast contact during rock glacier motion generates rock flour analogous to that produced through glacial

* Corresponding author. Fax: +1 802 443 2072.
E-mail address: jmunroe@middlebury.edu (J.S. Munroe).

0033-5894/$ – see front matter
http://dx.doi.org/10.1016/j.yqres.2012.12.006

erosion. Lake basins below rock glaciers, therefore, will receive a larger flux of fine clastic debris during episodes of rock glacier activity (Paasche et al., 2007). In addition, the climatic conditions responsible for rock glacier activity may enhance delivery of terrestrial material to lakes through soil creep and erosion by overland flow, perhaps aided by reduced vegetative cover. Intervals of cooler, periglacial climate should, therefore, be recognizable in sedimentary records of downstream basins as times of increased influx of physically weathered rock debris and colluvium (e.g., Armour et al., 2002).

This study investigated the Holocene history of rock glacier activity at a particular site in the Uinta Mountains of northern Utah (Fig. 1). Rock glaciers are common in the Uinta Mountains (Munroe and Laabs, 2009), and the site selected for this study is representative of the array of periglacial landforms common at high elevations throughout this part of the Rocky Mountains (e.g., Janke, 2007; Refsnider and Brugger, 2007). What makes this setting unique is a direct hydrologic connection between a complex of rock glaciers and a perennial lake that serves as a sediment sink. The lake was cored with the goal of generating a Holocene periglacial history that could be compared with other paleoclimate records from the region to identify commonalities and illuminate potential forcing mechanisms.

Setting

The Uinta Mountains are a major component of the Rocky Mountain system, produced by Laramide uplift of a thick sequence of Precambrian metasedimentary rocks known as the Uinta Mountain Group (Sears et al., 1982). Glaciers are not present in the Uintas today, but a rich geomorphic record of moraines indicates that flowing ice covered >2000 km^2 of the Uinta landscape during the LGM (Munroe and Laabs, 2009). Cosmogenic surface-exposure dating of moraine boulders using ^{10}Be, and ^{14}C dating of rock flour accumulation in a downstream lake, have demonstrated that the local LGM in the western Uintas occurred ca. 20 cal ka BP and that glaciers were present near their terminal positions until 18–16 cal ka BP (Laabs et al., 2009; Rosenbaum et al., 2012).

The site investigated for this project is located on the north slope of the range, 28 km south of the Utah–Wyoming border (Fig. 1). At this location, an extensive complex of talus, rock glaciers, and end moraines sprawls outward from the base of a steep, north-facing headwall at an elevation of ~3400 m (Fig. 2A). This complex covers an area of ~1 km^2 with an unknown thickness of quartzite rubble. Clasts range from large boulders (5 m in length) down to pebbles. The surficial layers of these deposits feature an openwork texture, although finer material at depth is revealed in local exposures.

At the northern extent of the complex, several prominent ridges arc from east to west, rising 3 to 15 m above the tundra surface (Fig. 1). A characteristic of these features is their superior height above neighboring block-covered regions to the south. Previous work interpreted these features as terminal moraines of extensively debris-covered glaciers (Munroe, 2002). There is, however, no clear dividing line between a debris-covered glacier and an ice-cored rock glacier (Clark et al., 1998). It is equally possible, therefore, that these features are the remnants of the latter, where the low-lying area behind the terminal ridge reflects collapse of a blocky surface as an ice core melted out. Fortunately, the determination of whether these outer ridges are terminal moraines from small cirque glaciers or collapsed ice-cored rock glaciers is not critical for accurately interpreting the lake sediment records described herein. The presence of either glaciers or rock glaciers as active geomorphic agents at this location would require conditions more periglacial than modern.

Between the outer ridges and the headwall lies the rest of the complex, which is dominated by rock glaciers and actively accumulating talus. The rock glaciers are revealed as wrinkles in a sea of rock debris, spectacularly highlighted by shadows at times of low solar angles, and by lingering snowdrifts that accumulate in the sinuous depressions (Fig. 2A). Each of these ridges has relief of ~2–10 m, and many are laterally continuous for >100 m. Without a dedicated, high-precision monitoring campaign it is impossible to determine

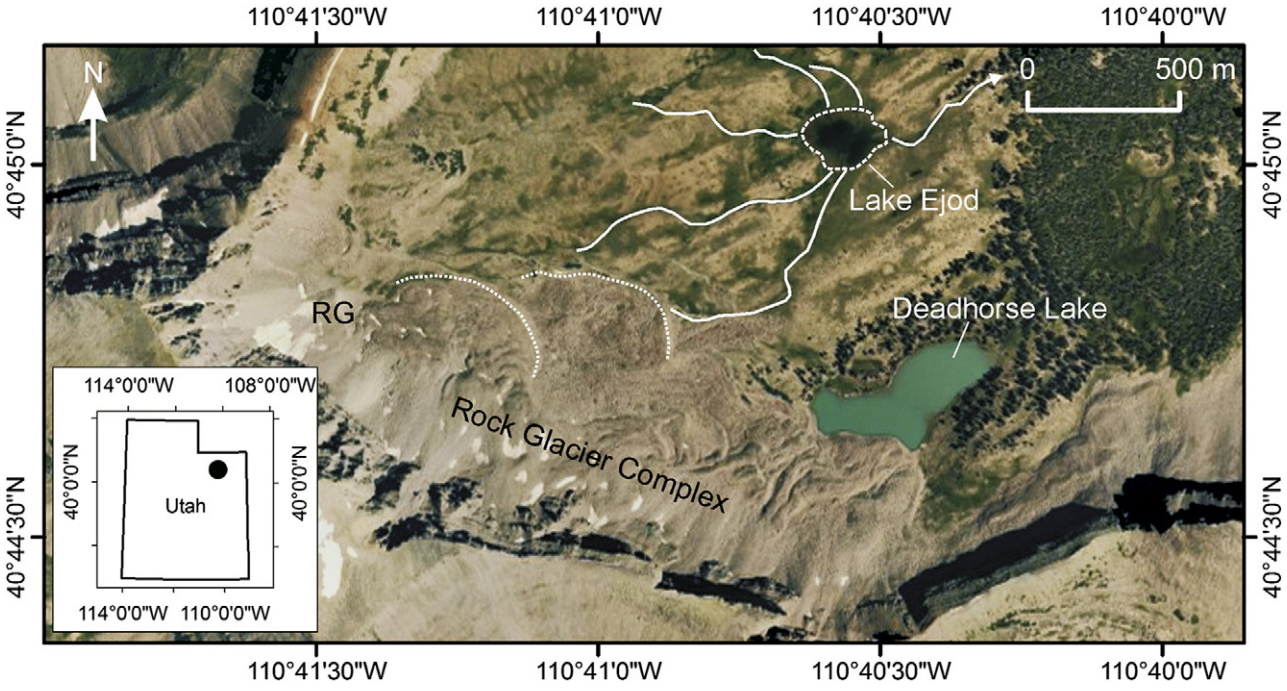

Figure 1. Location map for the Lake Ejod study area. Inset shows the state of Utah with a black circle marking the location of the study area. The large figure shows the position of Lake Ejod (dashed outline) and the extensive rock glacier complex to the south. Stream channels leading to Lake Ejod are highlighted with white lines. The most prominent terminal ridges of this complex, which were dated with lichenometry by Munroe (2002) are highlighted with dotted lines. "RG" marks the location of a modern rock glacier assumed to be active based on its morphology. Note the turquoise color of Deadhorse Lake, which currently receives rock glacier meltwater, in contrast to the clear water of Lake Ejod.

https://doi.org/10.1016/j.yqres.2012.12.006 Published online by Cambridge University Press

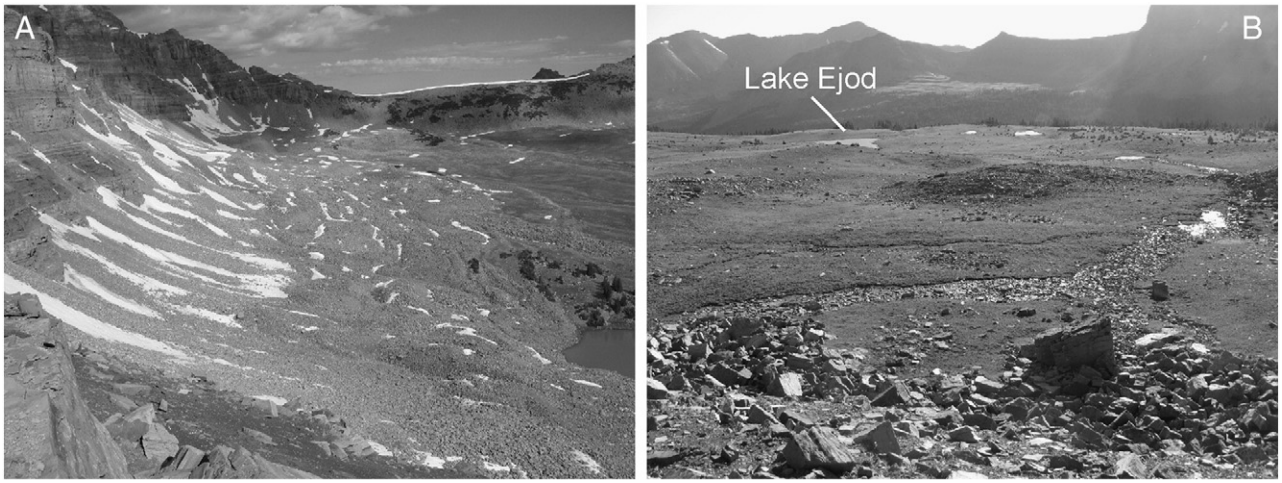

Figure 2. Views of the study area. Panel A shows a view westward across the rock glacier complex revealing the furrowed nature of the landforms. Panel B shows a view northeastward from the terminal ridge of the rock glacier complex following the path of a stream channel leading in an arc to Lake Ejod in the distance. The total length of this channel is 600 m.

whether any of these features is currently advancing. However, based on its sharp morphology and a perennial spring discharging water at a consistent temperature of 0°C, at least one lobe in the far southwestern corner of the cirque (Fig. 1) is likely active (Munroe, 2002).

From the rock glacier complex a series of cobble-floored channels leads directly into Lake Ejod (name taken from the Red Knob, Utah USGS 7.5′ quadrangle, Fig. 1). The main drainage originates where a pair of channels merges <50 m from the foot of the ridge that defines the northeastern boundary of the rock glacier complex (Fig. 2B). This combined channel then passes beneath a rock avalanche deposit before reemerging and winding its way northward to enter the southern end of Lake Ejod. The total length of this channel is ~600 m. Another, less well-defined channel leads eastward from the northern sector of the rock glacier complex, reaching Lake Ejod near the inlet from the main channel (Fig. 1). There is no geomorphic evidence that drainage from the rock glacier complex ever bypassed Lake Ejod in the post-glacial period. Thus, a history of past rock glacier activity should be preserved in the lacustrine sedimentary record.

Lake Ejod has a surface elevation of 3333 m and covers 2.7 ha to a maximum depth of 4.5 m. Stream channels also enter the lake from the west and north, originating in areas devoid of rock glaciers or extensive talus (Fig. 1). All of these channels connect with gullies cut into a shallow shelf that is submerged when the lake is overflowing. This relationship indicates that the lake has a history of water-level changes, which is confirmed by inspection of available aerial photography. Nonetheless, there is no evidence that the lake has ever desiccated completely. The lake drains eastward over an uneroded lip of glacial till that provides an upper limit on how high the water level can rise.

Lake Ejod is surrounded by a mosaic of alpine tundra, bare mineral soil, and exposed bedrock ledges. Krummholz and young trees (primarily *Picea engelmannii* and *Abies lasiocarpa*) exhibiting an upright growth form are scattered on the slopes surrounding the lake, but the lake sits ~10 m (250 m horizontally) above the limit of closed forest.

Methods

Field methods

Lake Ejod was cored (40° 45.047 N, 110° 40.578 W, WGS84) on August 12, 2005 from a floating platform anchored in 4.43 m of water. A combination of coring equipment was employed to retrieve a continuous stratigraphic sequence. A Livingstone corer fitted with a 5-cm-diameter clear polycarbonate core barrel was used to retrieve an intact sediment–water interface. This core was sampled at 1-cm intervals into Whirlpak bags. The Livingstone corer was then fitted with a 5-cm-diameter stainless steel barrel for two overlapping drives (A&B) that penetrated to a depth of 216 cm beneath the sediment–water interface. These cores were extruded, wrapped in saran and aluminum foil, and stored in divided core boxes for transport. Finally a 7.5-cm-diameter percussion corer was used to penetrate to the length of the core barrel (300 cm). Partial failure of the piston resulted in loss of some sediment, however the retrieved sediment still reached 23 cm below the base of Livingstone core B. The percussion core barrel was cut to ~80-cm lengths and capped for transport. After ground shipping back to Middlebury College, the cores were stored at 4°C until analysis.

Lab methods

The cores from Lake Ejod were analyzed for a variety of physical properties, primarily at 1-cm intervals. Livingstone and percussion core sections were run through a Bartington Magnetic Susceptibility (MS) meter connected to a sensor loop. The meter was re-zeroed every 50 cm, and corrections were applied for drift and for the different diameters of the Livingstone and percussion core sections. Properties of light reflected off the cleaned sediment surface were determined with a Konica-Minolta CM-2600D color spectrophotometer. Three measurements were averaged every cm. Color values were recorded using the CIELAB L*a*b* system where L* is luminosity from 0 (black) to 100 (white), a* is a measure of redness (positive values) to greenness (negative values), and b* is a measure of yellowness (positive values) to blueness (negative values). Bulk density (BD) was determined using a known-volume sampler (3 cm^3) and oven-dried samples. Thermogravimetric analysis was conducted with a Leco TGA-701. Water content was determined by drying at 105°C under nitrogen, while organic matter (OM) was estimated by combustion at 550°C under ambient atmosphere (Dean, 1974). C:N was measured with a Thermo Fisher Flash 2000 Elemental Analyzer. The analyzer was calibrated with aspartic acid, and standard reference materials were run every ~30 samples. Precision of the analyzer is approximately 1% for C and 0.5% for N. Grain-size distribution (GS) was measured with laser scattering in a Horiba LA950 after pretreatment with 35% H_2O_2 (3 additions of 10 ml over 7–10 days) to remove organic matter and 0.1 M NaOH (1 h, 85°C) to remove biogenic silica. Sodium hexametaphosphate (3%) was used as a dispersant and all samples were sonified and mechanically mixed before analysis. A

https://doi.org/10.1016/j.yqres.2012.12.006 Published online by Cambridge University Press

refractive index of 1.54 with an imaginary component of 0.1i was used for the calculations. 10% of samples were rerun as duplicates. The abundance of biogenic silica (bSi) was determined through sequential extraction (5 hourly extractions) in 0.1 M NaOH in a shaker bath at 85°C. After addition of reagents for a molybdate blue reaction (Strickland and Parsons, 1965), the concentration of dissolved silica was determined through spectrophotometry against a 10-sample standard curve. Analysis of replicates indicates that this method has a reproducibility of ~10% (Munroe, 2012).

Quantification of phosphorus fractions was performed at 2-cm spacing with sequential extraction (Filippelli et al., 2006). Oven-dried, ground samples were leached in citrate dithionite bicarbonate, and ICP-AES was used to determine the iron-bound (Fe-P) P concentration in the leachate. Authigenic/biogenic P was then removed with Na-acetate, and mineral P (mP) was removed with HCL. Finally, organic P was isolated with $MgNO_3$. Spectrophotometry was used to determine the P concentrations in the last three extractions, and authigenic/biogenic and organic P concentrations were summed to yield org-P. Fe-P is considered to represent soil erosion into the lake, org-P represents primary productivity within the lake, and mP represents erosion of physically weathered bedrock in the watershed (Filippelli et al., 2006). Random duplicates were run for 15% of the samples.

Terrestrial macrofossils were removed from the core for AMS ^{14}C dating at Beta Analytic. These were rinsed and stored in distilled water until analysis. The resulting ^{14}C dates were calibrated into calendar years (cal yr) BP using Calib 6.0 (Stuiver and Reimer, 1993) and the IntCal09 calibration curve (Reimer et al., 2009).

Results

Stratigraphy

The sediments in Lake Ejod are primarily dense, reddish silty clay, locally interrupted by pink clay-rich layers and layers rich in diffuse organic matter, both usually <1 cm thick. There is a general progression to darker brown hues with depth. The exception to this consistent stratigraphy is a 14-cm-thick layer of sand (median GS of ~200 μm) encountered at a stratigraphic depth of 163–176 cm in both Livingstone core B and the percussion core. The upper and lower contacts of this unit are abrupt, and the sand contains very little organic matter (<2%) and <3% clay (Fig 3). The coarse grain size indicates that this layer represents a high-energy event that occurred only once in the time interval represented by the core. A flood could explain the coarse sediment, but a high-energy flow along one of the stream channels leading to the lake would transport a mixture of clastic debris, terrestrial organic matter, and eroded soil, whereas the layer is distinctly devoid of organic components and fines. A more likely interpretation is that this layer was produced by a slushflow (Washburn and Goldthwait, 1958) that transported a slurry of sandy debris from the headwall across the snow surface to rest on the lake ice. This mechanism explains the coarse grain size and lack of organic material, and dumping of this material to the lake bottom as the ice melted would explain the abrupt bounding contacts.

The known overlaps of the Livingstone and percussion core sections, along with pink layers and other stratigraphic markers, supported stacking of the four cores into a single stratigraphic sequence. Physical properties measured at 1-cm intervals provided an additional check on the construction of this composite record (Fig. 3). Values within the zones of overlap were averaged to smooth transitions between core sections, and the 14-cm-thick sand layer was removed, given the interpretation that it represents an instantaneous event. The resulting composite record extends from the sediment–water interface to a depth of 239 cm below the lake floor.

Geochronology and age model

Four samples of conifer needles submitted for AMS ^{14}C dating returned ages in correct chronostratigraphic order (Table 1). Calibration of these results into calendar years BP yields ages from ~5200 cal yr BP for the deepest sample (19 cm above the base of the core), to 600 cal yr BP (at a depth of 38 cm). A depth-age model was created by fitting a second-order polynomial ($r^2 = 0.999$) to the median probabilities of the calibrated age ranges for these samples, along with an age of −55 cal yr BP (AD 2005) for the sediment–water interface (Fig. 4). Extrapolating using this model, the base of the core dates to 5330 cal yr BP. Local sedimentation rates range from 0.3 to 0.6 mm/yr, and the 1-cm interval at which most analyses were made corresponds to 17 to 31 yr.

Analytical results

Time series of data measured in this study are presented in Figure 5 on a common timeline in cal yr BP. Raw data are shown as points, along with lines representing smoothed time series calculated with a Gaussian function and filled relative to mean values. Many data series exhibit long-term changes over the 5300-year record. For instance, organic matter, water, and bSi are consistently above their means before ~3500 cal yr BP, and generally fall over time. Other properties, including L*, BD, and mP are consistently below mean

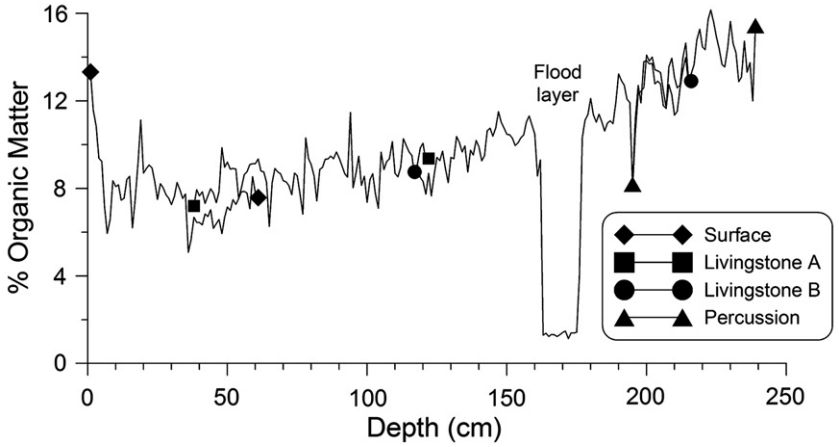

Figure 3. Organic matter concentration in the four cores (surface, Livingstone A&B, and percussion) stacked to assemble the composite stratigraphic sequence for Lake Ejod. Paired symbols mark the top and bottom values in each core section. Clearly visible overlaps were used to align the individual cores. The coarse, organic-poor flood layer is also obvious. This was assumed to represent an instantaneous event and was removed from the stratigraphy before application of the depth-age model.

https://doi.org/10.1016/j.yqres.2012.12.006 Published online by Cambridge University Press

Table 1
Radiocarbon dates for the Lake Ejod core.

Lab #	Sample name	Depth[a] cm	^{14}C age yr	^{13}C/^{12}C‰	Calibration ranges[b] yr BP
257443	EJOD-1	38	630 ± 40	−23.5	**549–665 (1.000)**
257444	EJOD-2	94	1870 ± 40	−25.5	**1712–1890 (1.000)**
257445	EJOD-3	180	3640 ± 50	NA	**3836–4090 (0.994)**, 4132–4137 (0.006)
257446	EJOD-4	220	4560 ± 40	−19	**5051–5192 (0.550)**, 5213–5322 (.406), 5419–5440 (0.044)

NA indicates sample was too small for ^{13}C/^{12}C analysis.
[a] After removal of flood layer from 163 to 176 cm.
[b] Bold highlights most probable age range.

values before 3500 cal yr BP and rise over time. These changes record a long-term transition from dark, organic-rich, relatively low-density sediment, to denser, less organic sediment containing an increasing component of freshly weathered bedrock. In contrast to these long-term trends, C:N exhibits a major drop from ~18 to ~12 at ca. 4000 cal yr BP.

Between 3200 and 1000 cal yr BP, time series of VF silt, median GS, and mP exhibit a series of pronounced oscillations. Values of VF silt and mP are notably above average, and median GS below average, in three intervals: 3200–2600, 2300–2000, and 1800–1000 cal yr BP (Fig. 5). Thus, the sediment accumulating in Lake Ejod during these intervals was unusually rich in fine clastic material. Converting values of VF silt and mP to z-scores and summing them yields a composite time series that clearly delineates these intervals and allows their correspondence with other physical properties to be evaluated (Fig. 5). These relationships are variable at shorter time scales, however these three intervals fall within a long stretch of falling values of organic matter, water content, and bSi, and rising values of a*, BD, and clastic material. Thus, the sediment accumulating in Lake Ejod during these three intervals was unusually rich in dark red silt, and relatively depleted in organic matter and byproducts of autochthonous productivity. Several prominent layers of pink clay-rich sediment noted in the visual stratigraphy also fall within these intervals, and thin organic-rich layers generally cluster in between them, suggesting a lake alternating between productive and clastic-dominated states (Fig. 5).

The last several centuries feature notable proxy shifts in slightly different combination (Fig. 5). From 500 to 300 cal yr BP median GS is low and VF silt is high, similar to the three intervals noted earlier. However values of mP are only slightly elevated, a* temporarily decreases, and L* is relatively high. Thus, the sediment that accumulated during these two centuries was fine and dense, but less rich in mP and less red in hue.

Finally, the last century, represented by the uppermost 5 cm of the composite record, witnessed extreme values in several data series (Fig. 5). Abundance of organic matter rose to >13%, which is the highest level since ~5000 cal yr BP. Abundance of bSi rose even more dramatically to 11%, which is by far the highest value in the entire record. And C:N dropped to <9, a record low that is particularly striking given the relatively stable values that persisted for the previous 4000 years.

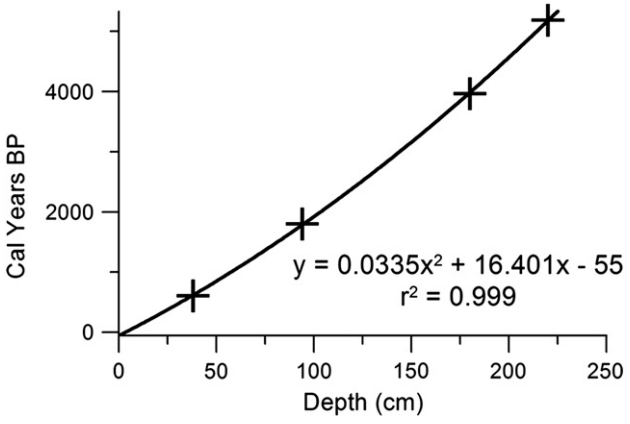

Figure 4. Depth-age model for Lake Ejod based on four AMS ^{14}C dates determined on conifer needles (see Table 1).

Discussion

Interpretive framework

Given the proximity and direct hydrologic connection of Lake Ejod to an extensive complex of talus, rock glaciers, and end moraines, downcore variations in physical properties likely record processes responsible for the formation of this complex. If glaciers were active upstream from Lake Ejod during the time represented by the composite sediment core, then they would have generated fine-grained rock flour through abrasion that would have been available for transport downstream to the lake (e.g., Leonard, 1997; Rosenbaum and Reynolds, 2004). However, evidence for active glaciers above Lake Ejod during the last 5300 years is equivocal. A more likely sediment source is the rock glaciers, which would also generate fine clastic sediment through crushing and mechanical weathering of rocks during forward motion. Prior studies have used variations in fine sediment abundance in lake sediment cores as evidence of upstream rock glacier activity (e.g., Paasche et al., 2007). Moreover, modern lakes in the Uinta Mountains that receive meltwater directly from rock glaciers exhibit a distinct turquoise blue color, consistent with abundant fine suspended sediment. Analysis of the grain-size distribution of surface (i.e. modern) sediment in two of these lakes (including Deadhorse Lake, Fig. 1), reveals that they are dominated by very fine and fine silt. In contrast, Lake Ejod, which does not currently receive significant meltwater from rock glaciers, has clear water (black in Fig. 1), and surface sediment with a larger proportion of coarse and medium silt. Thus, the abundance of very fine and fine silt is a viable proxy for past rock glacier activity.

Other physical properties measured in this study would change in predictable ways with varying rock flour influx. For instance, physically weathered clastic debris should exhibit a larger fraction of mP than soil or terrestrial organic matter (Filippelli et al., 2006). Similarly, because much of the bedrock surrounding Lake Ejod has a dark reddish hue, increased rock flour entering the lake would promote higher values of a* and lower values of L*. Depression of organic matter and bSi values would be expected during intervals of high rock flour influx, either because of dilution of these constituents by increased clastic input (e.g., Kaplan et al., 2002), or because of actual reductions in their production by the climatic conditions that encouraged rock flour production. Collectively, therefore, centennial-scale intervals of the Lake Ejod core featuring greater abundance of fine-grained, dark red, clastic sediment rich in mP and depleted values of OM and bSi are interpreted as times of elevated rock flour influx from upstream rock glaciers. Random fluctuations of these variables at shorter temporal scales are expected given that different channels leading to the lake, and different sectors of the rock glacier complex (Fig. 1), may have been active at different times, and that the color of the Uinta Mountain Group bedrock varies through the stratigraphy exposed above Lake Ejod.

Because glaciers and (widespread) active rock glaciers are absent from the watershed of Lake Ejod today, increased glacial or periglacial activity in the past would require cooler temperatures that created a positive mass balance for surface (glacial) and subsurface (permafrost) ice. Cooler temperatures may also have increased the frequency of freeze–thaw cycles, enhancing talus accumulation and further

https://doi.org/10.1016/j.yqres.2012.12.006 Published online by Cambridge University Press

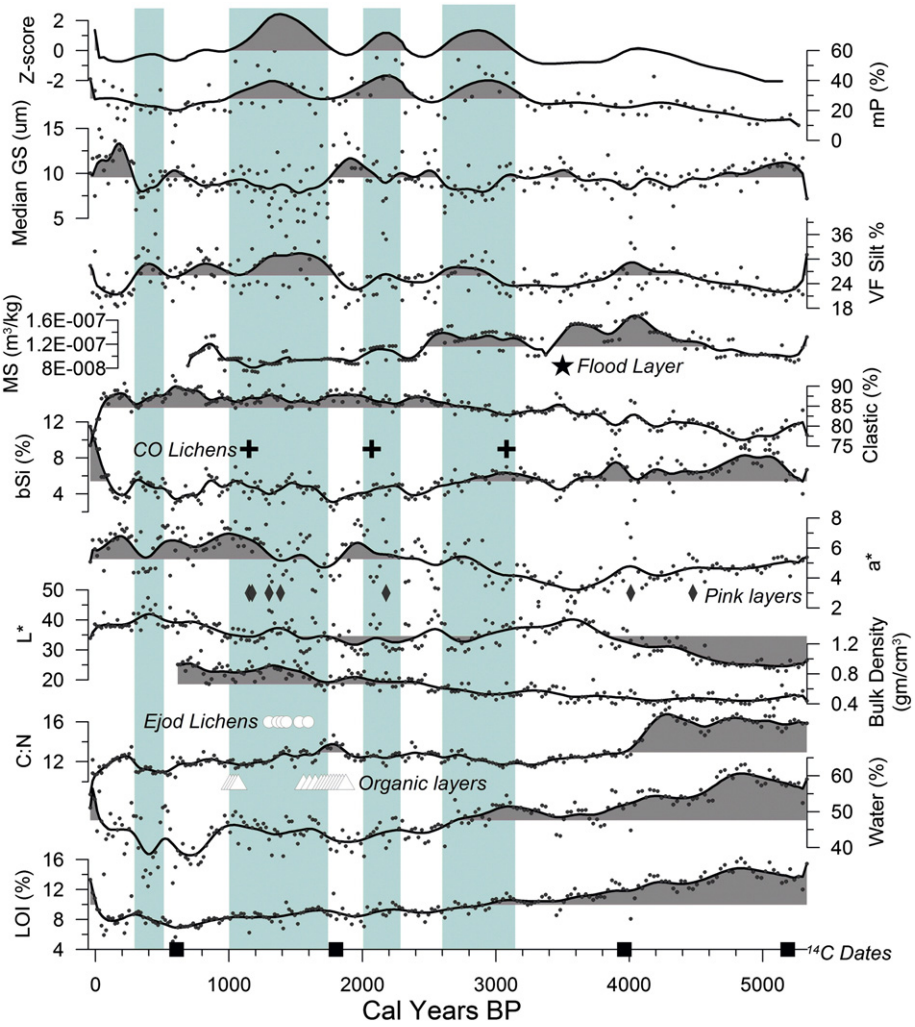

Figure 5. Biogeochemical properties measured in the Lake Ejod composite record displayed as time series in cal yr BP. Raw values are presented as individual points. Smoothed time series, generated with a Gaussian function, are displayed as thicker lines filled relative to their mean values. LOI is organic matter determined by loss-on-ignition at 550°C. L* and a* are color values presented in the CIELAB system. Clastic content was determined by subtracting OM and bSi from 100. MS is mass specific magnetic susceptibility. VF Silt is very fine silt (7–2 μm). mP is mineral P after Filippelli et al. (2006). Lichen dates were determined on the rock glacier complex upstream from Lake Ejod (Munroe, 2002). Organic layers and pink layers were noted in the visual stratigraphy of the cores. The location of the flood layer, which was removed from the time series, is marked with a star. Z-score refers to the time series generated by summing the z-scores of VF silt and mP. Gray rectangles outline inferred episodes of periglacial activity delineated by the z-score time series.

encouraging the formation and persistence of rock glaciers. Thus, the sedimentary record of Lake Ejod is considered a climatic history in which periglacial activity was enhanced during times of cooler temperatures. For clarity, these intervals will be referred to simply as times of increased periglacial activity, with the understanding that ice glaciers may have played a role in some of them.

Other possible interpretative frameworks fail to explain the shifts seen in the suite of proxies, or are unlikely given the physical setting. Prolonged changes in water level, for instance, could impact the amount of organic matter accumulating at the coring site by changing the position of the littoral zone (e.g., Shuman, 2003). However, the outlet threshold of the lake is not incised, indicating that the water level has not fallen substantially over time, and that the modern, overflowing level represents the long-term maximum. Similarly, the subaqueous channels projecting from the inlet streams indicate that the water level does drop occasionally. However, changes seen in down-core stratigraphic records greatly surpass the variability measured in the recent sediment, even though aerial photographs document short-lived, seasonal drops in water level. These temporary water level changes are, therefore, insufficient to explain the sustained shifts evident in the data series. Furthermore, consistently low water over decadal timescales is unlikely given the hydroclimate of the Lake Ejod watershed. The annual precipitation at this elevation (likely ~100 cm/yr, based on nearby SNOTEL data) and large watershed-to-lake area ratio (70:1) generates a potential runoff volume >30× larger than the lake volume, meaning that conditions would need to have been unrealistically dry for multiple consecutive years in order to stabilize Lake Ejod at a significantly lower level.

Another possibility is that reduced precipitation might diminish stream power, shifting the clastic load accumulating in Lake Ejod to a finer median GS. However, the abundance of clastic material is higher in the latter part of the record when median GS is low, which is inconsistent with reduced inputs. Conversely, increased precipitation could deliver coarser sediment to the lake, but would also be expected to wash in additional terrestrial organic matter (leading to higher C:N and organic matter abundance). Yet there is no consistent relationship between coarser median GS size and the other physical properties, and intervals of coarser GS correspond to lower values of mP, suggesting a lower clastic influx.

It is also conceivable that the fine sediment in the Lake Ejod record is eolian dust, rather than rock flour. Alpine and subalpine soil profiles in the Uintas contain a ubiquitous cap of alpine loess, indicating accumulation of eolian sediment during the post-glacial period (Bockheim and Koerner, 1997; Bockheim et al., 2000; Munroe, 2007). More

https://doi.org/10.1016/j.yqres.2012.12.006 Published online by Cambridge University Press

recent work has documented effects of eolian additions to subalpine watersheds (Moser et al., 2010; Reynolds et al., 2010), and grain-size analysis reveals that modern dust accumulating in the Uintas has a mode of very fine silt, similar the rock flour produced by rock glaciers (Munroe, unpublished). Given these observations, variations in the abundance of VF silt in the Lake Ejod record could reflect changes in the rate of eolian dust delivery over time. However, synchronous fluctuations in VF silt abundance are not obvious in grain-size records from other Uinta lakes. Therefore, although dust is likely a component of the sediment in Lake Ejod, dust accumulation is apparently overprinted by other local mechanisms responsible for delivering VF silt to the lake. Overall, therefore, the interpretation that elevated fine-sediment influx is a signal of increased rock flour production during cooler intervals with enhanced periglacial activity offers the most consistency across the suite of available proxies.

Periglacial history

Although the Lake Ejod record only covers the latter half of the Holocene, the long-term transition to more frequent intervals of periglacial activity in the watershed implies the operation of a millennial-scale climate driver. A likely candidate is decreasing summer insolation, which peaked for this latitude ca. 10 cal ka BP at 110% of modern values and decreased steadily throughout the Holocene (Berger, 1978). This long-term change resulted in cooler summers after the Altithermal in the early-middle Holocene (Antevs, 1948). Effects of the Altithermal and post-Altithermal transition in the Uinta Mountains have been noted in pollen data indicating higher treeline in the early Holocene and a period of maximum warmth ca. 5500 cal yr BP (Munroe, 2003). The long-term transition seen in the Lake Ejod sediment, therefore, may record the cooling climate that followed the Altithermal. In this scenario, the organic-rich, low-density sediment with high bSi and C:N that accumulated before ~3500 cal yr BP represents a productive aquatic environment surrounded by a watershed that supported at least local forest cover. Steady reduction in the productivity of this environment, in response to decreasing summer insolation and cooler temperatures, is represented by the falling values of organic matter and water content, and rising values of BD, signifying a larger proportion of clastic material in the sediment.

Given that treeline is currently below Lake Ejod, the major drop in C:N ca. 4000 cal yr BP (Figs. 5 and 6) likely represents the time at which treeline fell below the lake and extensive forests abandoned the watershed, shifting from higher C:N values indicative of terrestrial organic matter to lower values signifying aquatic organic matter (Meyers and Ishiwatari, 1993). This change coincides with shifts toward lighter sediment color (higher L* values), and lower bSi and OM suggesting that productivity of the lake was reduced in this new alpine setting. Scattered trees similar to those on the modern landscape must still have been present in the watershed because the ^{14}C dates were determined on conifer needles. However, C:N values never rebounded after 4000 cal yr BP (Fig. 5), strongly suggesting that closed forest remained below the lake for the remainder of the record.

In this context of decreasing insolation, falling treeline, and a slow transition toward cooler conditions, the first major rise in mP abundance ca. 3200 cal yr BP represents the start of extensive periglaciation in the watershed above Lake Ejod (Figs. 5 and 6). This rise coincides with a drop in median GS, an increase in the abundance of VF silt, and a shift in sediment color toward a darker red hue (lower L*, higher a*), all of which are consistent with increased delivery of rock flour of the lake. The timing of this event matches a periglacial episode in the Sangre de Cristo Mountains of northern New Mexico (Armour et al., 2002), as well as the onset of Neoglaciation in the eastern Sierra Nevada (Fig. 6) inferred from analysis of rock flour in lacustrine sediment cores (Bowerman and Clark, 2011). Other evidence for glacial activity ca. 3000 cal yr BP comes from sediment cores in northern Montana (Munroe et al., 2012) and moraine sequences in the Canadian Rockies (Clague et al., 2009). Global compilations have also noted widespread evidence for climate variability at this time, including clustering of rapid change events from 3500 to 2500 cal yr BP (Mayewski et al., 2004) and cooler conditions from 3300 to 2500 cal yr BP (Wanner et al., 2011). Together, this broad synchrony implicates a global climate forcing that promoted glacial and periglacial activity at this time (Fig. 6). The driver behind this change is unknown, however the timing coincides with a prominent minimum in solar activity (Steinhilber et al., 2009; Wanner et al., 2011), as well as an increase in ice-rafting in the North Atlantic (Bond et al., 1997), suggesting an internal feedback that amplified solar forcing.

The two younger intervals (2300–2000 and 1800–1000 cal yr BP) of elevated rock flour influx can also be interpreted as pulses of enhanced periglacial activity, forming a series of three episodes between 3200 and 1000 cal yr BP (Figs. 5 and 6). The timing of these is notable for its striking synchrony with episodes of rock glacier activity in Colorado. Using lichenometry, it was concluded that rock

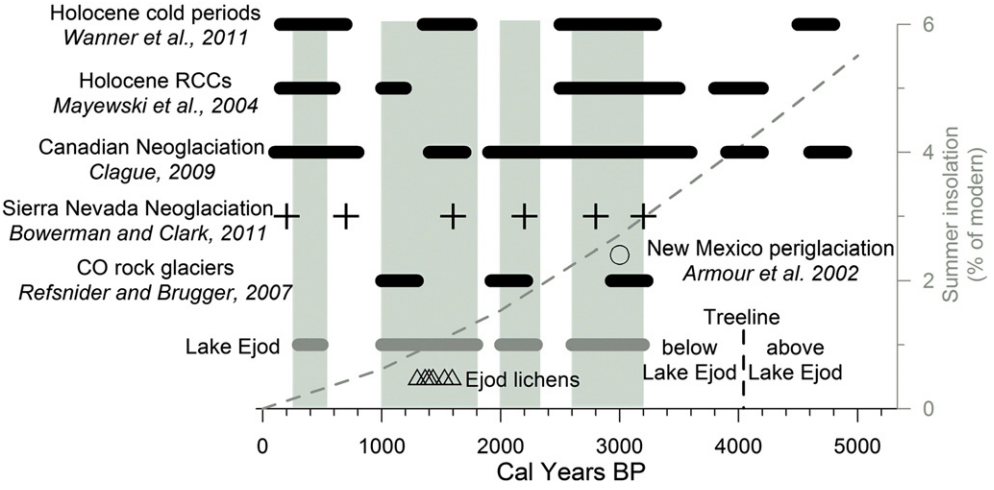

Figure 6. Comparison of the Lake Ejod periglacial record with other paleoclimate records from western North America. Gray rectangles outline the periglacial episodes identified in Fig. 5. Triangles represent the lichenometric ages determined for part of the rock glacier complex by Munroe (2002). The circle notes an episode of inferred periglaciation in the Sangre de Christo Mountains of northern New Mexico (Armour et al., 2002). The crosses mark episodes of Neoglacial activity inferred from lacustrine sediment in the Sierra Nevada (Bowerman and Clark, 2011). RCCs are rapid climate changes identified in a compilation of multiple paleoclimate records from around the globe (Mayewski et al., 2004). Summer insolation for 40°N north is from Berger (1978).

https://doi.org/10.1016/j.yqres.2012.12.006 Published online by Cambridge University Press

glaciers in the Sawatch Range were active ca. 3080, 2070, and 1150 cal yr BP (Refsnider and Brugger, 2007), which matches well with the midpoints of the periglacial intervals above Lake Ejod (2900, 2150, and 1400 cal yr BP) (Fig. 6). Even though these studies used distinctly different data sources to reconstruct past periglacial activity, the convergence of their conclusions is compelling evidence for synchronously oscillating periglacial climate in this region during the late Holocene.

Additional support for the record from Lake Ejod comes from lichenometry applied to the bouldery ridges at the head of the channels leading to the lake (Munroe, 2002) (Fig. 1). Measurement of the largest lichens on these ridges, and application of the lichen growth rate curve utilized by Refsnider and Brugger (2007), which was derived from Benedict (1993), yields ages from 1600 to 1300 cal yr BP, overlapping with the third periglacial interval inferred from Lake Ejod (Figs. 5 and 6). The most straightforward interpretation of this convergence is that the ridges closest to Lake Ejod, where lichens were measured, formed at this time. Alternatively, lichens that grew on these ridges before the third interval may have been eliminated by harsh conditions or rock overturning at this time, limiting the maximum age of measured lichens to 1600 cal yr BP even if parts of the complex are older.

A possible challenge to this interpretation is provided by recently generated cosmogenic surface-exposure ages determined for the same ridges that were dated with lichenometry by Munroe (2002). Inventories of ^{10}Be suggest that these ridges have been exposed to cosmic radiation since the latest Pleistocene (Marcott, 2011). If these dates are accurate, it requires that the rock flour that accumulated in Lake Ejod during the late Holocene originated from higher talus and rock glaciers closer to the headwall (Figs. 1 and 2), which necessitates a minor alteration to the interpretation presented above. It is difficult, however, to explain the order-of-magnitude difference between the lichen ages on these ridges and their apparent exposure ages. Perhaps snowkill events (e.g., Benedict, 1993) during the late Holocene have limited the maximum age of lichens on these features, and the apparent synchrony between the lichen ages and the third rock flour spike is mere coincidence.

The final interval of elevated rock flour ca. 500–300 cal yr BP coincides with the Little Ice Age (LIA) (Grove, 2004). The reduced water content (i.e., increased density) and elevated silt content of the sediment at this time is consistent with a greater rock flour influx. The significance of the lower a* values compared with older periglacial intervals is unclear, however the drop in a* is mirrored by a similar decrease in b* values (not shown in Fig. 5) indicating that the sediment became less yellow at the same time it became less red. This synchronous change suggests that rock flour was reaching Lake Ejod from a new source layer in the Uinta Mountain Group, either due to evolution of the channel network connected to the lake, or formation of a new periglacial feature. No matter what the explanation, the lichen ages indicate that the outer ridges of the rock glacier complex have been stable for more than a millennium, thus the LIA rock flour must have originated farther to the south, likely from the jumble of rock glacier lobes and talus cones that extends southward to the headwall (Fig. 1). This interpretation of periglacial, as opposed to glacial, activity during the LIA is consistent with a previous study which concluded that the LIA in the Uintas was marked by rock glacier activity (Munroe, 2002). Even though the LIA featured the most extensive glacial advances of the Neoglaciation in other parts of the Rocky Mountains, signifying the most profound excursion toward cooler conditions in the Holocene, paleohydrologic reconstructions suggest that the Uinta Mountains were relatively dry during this time (Carson and Munroe, 2005; Carson et al., 2007). Cool temperatures combined with dry conditions would encourage formation of rock glaciers rather than features composed entirely of ice.

Although the LIA may have been shorter than the periglacial intervals that preceded it, the midpoints of these four (2900, 2150, 1400, and 400 cal yr BP) suggest a cyclic oscillation in the severity of periglacial conditions (Figs. 5 and 6). Spectral analysis of the mP time series using Redfit (Schulz and Mudelsee, 2002) reveals a spectral peak of 885 yr within a band from 1050 to 750 yr that is significant at the 95% confidence interval. This period is close to the ~1000-yr cyclicity noted in varved records from the Santa Barbara Basin off the southern coast of California, and to similar variability of δ^{18}O in the GISP2 ice core, which have been correlated to solar cycles through their coherence with atmospheric ^{14}C abundance (Nederbragt and Thurow, 2005). The timing of periglacial intervals above Lake Ejod, therefore, is consistent with the growing body of evidence supporting a solar control over periodic Holocene climate variability.

Finally, the shifts in biogeochemical data in the 20th century are notable for their unprecedented magnitude (Fig. 5). The great increases in organic matter and bSi content, coupled with the major drop in C:N, imply a significant enhancement of aquatic productivity. Other studies in the western U.S. have noted shifts in high-elevation ecosystems in response to atmospheric delivery of nitrogen (Williams et al., 1996), and recent changes in the diatom assemblages of high-elevation Uinta lakes have been attributed to atmospheric metal deposition (Moser et al., 2010). The changes in the Lake Ejod record may be an additional manifestation of these processes in the Uinta Mountains. The tundra covered benches surrounding Lake Ejod also have been subjected to sheep grazing since the late 1800s (D. Koerner, US Forest Service, personal communication), and soil erosion and enhanced P cycling related to this land use may be responsible for some of the observed changes.

Conclusions

Multiproxy analysis of a sediment core from Lake Ejod in the northern Uinta Mountains supports development of a periglacial history spanning the past 5300 years. A direct hydrologic connection between an extensive rock glacier complex and the lake ensures that fluctuations in the production and delivery of rock flour, driven by climate changes, are recorded in the lake sediment. Given the setting of the lake and properties of the surrounding bedrock, shifts toward finer, denser, redder, and less organic sediment with a higher fraction of mineral P are interpreted as signals of enhanced periglacial activity. The early part of this record (before ~3500 cal yr BP) tracks deteriorating climatic conditions and falling treeline. The first of four major pulses in rock flour delivery began at 3200 cal yr BP, signifying the start of widespread periglaciation in the cirque above Lake Ejod. The timing of this inception matches periglacial and Neoglacial episodes elsewhere in the western U.S. (e.g., Armour et al., 2002; Bowerman and Clark, 2011). Two younger periglacial intervals form a triplex that matches lichenometrically determined ages of rock glacier activity in the Colorado Rockies (Refsnider and Brugger, 2007), providing compelling evidence for a cyclically oscillating periglacial climate in this region during the latter half of the Holocene. The last of these three intervals, 1800–1000 cal yr BP overlaps with ages (1600–1300 cal yr BP) determined for lichens on rock glacier ridges above Lake Ejod using the same growth rates applied in the Colorado study (Munroe, 2002). This convergence suggests that the outer part of the rock glacier complex was constructed around this time. Periglacial activity during the Little Ice Age (Grove, 2004) is represented by a pulse in rock flour influx from 500 to 300 cal yr BP. This sediment exhibits a median grain size matching that of the previous three intervals but has a slightly different color and mineral P content, suggesting that a new source of rock flour was connected to the lake at this time. Finally, dramatic changes in several biogeochemical measures indicate an unprecedented surge in aquatic productivity during the 20th century, which may reflect atmospheric N deposition (Williams et al., 1996) and the effects of livestock grazing in the Lake Ejod watershed.

https://doi.org/10.1016/j.yqres.2012.12.006 Published online by Cambridge University Press

Acknowledgments

Funding was provided by NSF EAR-0345112 to J. Munroe. C. Klem received support from the Middlebury College Senior Work Fund. The field assistance of M. Devito, K. Moser, N. Oprandy, C. Plunkett, D. Porinchu, and B. White is greatly appreciated. Comments of K. Brugger, J. Knox, and an anonymous reviewer were helpful in improving the manuscript.

References

Antevs, E.V., 1948. The Great Basin, with emphasis on glacial and postglacial times: climatic changes and pre-white man. Bulletin of the University of Utah 38, 168–191.
Armour, J., Fawcett, P.J., Geissman, J.W., 2002. 15 k.y. paleoclimatic and glacial record from northern New Mexico. Geology 30, 723–726.
Benedict, J.B., 1967. Recent glacial history of an alpine area in the Colorado Front Range, USA. I. Establishing a lichen-growth curve. Journal of Glaciology 6, 817–832.
Benedict, J.B., 1993. A 2000-year lichen-snowkill chronology for the Colorado Front Range, USA. The Holocene 3, 27–33.
Berger, A.L., 1978. Long-term variations of caloric insolation resulting from the Earth's orbital elements. Quaternary Research 9, 139–167.
Bockheim, J., Koerner, D., 1997. Pedogenesis in alpine ecosystems of the eastern Uinta Mountains, Utah, USA. Arctic and Alpine Research 164–172.
Bockheim, J., Munroe, J., Douglass, D., Koerner, D., 2000. Soil development along an elevational gradient in the southeastern Uinta Mountains, Utah, USA. Catena 39, 169–185.
Bond, G., Showers, W., Cheseby, M., Lotti, R., Almasi, P., Demenocal, P., Priore, P., Cullen, H., Hajdas, I., Bonani, G., 1997. A pervasive millennial-scale cycle in North Atlantic Holocene and glacial climates. Science 278, 1257–1266.
Bowerman, N.D., Clark, D.H., 2011. Holocene glaciation of the central Sierra Nevada, California. Quaternary Science Reviews 30, 1067–1085.
Carson, E.C., Munroe, J.S., 2005. Tree-ring based streamflow reconstruction for Ashley Creek, northeastern Utah: implications for palaeohydrology of the southern Uinta Mountains. The Holocene 15, 602–611.
Carson, E.C., Knox, J.C., Mickelson, D.M., 2007. Response of bankfull flood magnitudes to Holocene climate change, Uinta Mountains, northeastern Utah. Geological Society of America Bulletin 119, 1066–1078.
Clague, J.J., Menounos, B., Osborn, G., Luckman, B.H., Koch, J., 2009. Nomenclature and resolution in Holocene glacial chronologies. Quaternary Science Reviews 28, 2231–2238.
Clark, D.H., Steig, E.J., Potter Jr., N., Gillespie, A.R., 1998. Genetic variability of rock glaciers. Geografiska Annaler: Series A, Physical Geography 80, 175–182.
Davis, P.T., Menounos, B., Osborn, G., 2009. Holocene and latest Pleistocene Alpine glacier fluctuations: a global perspective. Quaternary Science Reviews 28, 2021–2033.
Dean Jr., W.E., 1974. Determination of carbonate and organic matter in calcareous sediments and sedimentary rocks by loss on ignition; comparison with other methods. Journal of Sedimentary Petrology 44, 242–248.
Filippelli, G.M., Souch, C., Menounos, B., Slater-Atwater, S., Jull, A.J.T., Slaymaker, O., 2006. Alpine lake sediment records of the impact of glaciation and climate change on the biogeochemical cycling of soil nutrients. Quaternary Research 66, 158–166.
Grove, J.M., 2004. Little Ice Ages; Ancient and Modern. Routledge, London, UK (718 pp.).
Janke, J.R., 2007. Colorado Front Range Rock Glaciers: distribution and topographic characteristics. Arctic, Antarctic, and Alpine Research 39, 74–83.
Kaplan, M.R., Wolfe, A.P., Miller, G.H., 2002. Holocene environmental variability in southern Greenland inferred from lake sediments. Quaternary Research 58, 149–159.
Laabs, B.J.C., Refsnider, K.A., Munroe, J.S., Mickelson, D.M., Applegate, P.J., Singer, B.S., Caffee, M.W., 2009. Latest Pleistocene glacial chronology of the Uinta Mountains: support for moisture-driven asynchrony of the last deglaciation. Quaternary Science Reviews 28, 1171–1187.
Leonard, E.M., 1997. The relationship between glacial activity and sediment production; evidence from a 4450-year varve record of neoglacial sedimentation in Hector Lake, Alberta, Canada. Journal of Paleolimnology 17, 319–330.
Marcott, S.A., 2011. Late Pleistocene and Holocene Glaciers and Climate Change. Unpublished Ph.D. dissertation, Oregon State University, 248 pp.
Mayewski, P.A., Rohling, E.E., Stager, C.J., Karlen, W., Maasch, K.A., Meeker, L.D., Meyerson, E.A., Gasse, F., van Kreveld, S., Holmgren, K., Lee-Thorp, J., Rosqvist, G., Rack, F., Staubwasser, M., Schneider, R.R., Steig, E.J., 2004. Holocene climate variability. Quaternary Research 62, 243–255.
Meyers, P.A., Ishiwatari, R., 1993. Lacustrine organic geochemistry; an overview of indicators of organic matter sources and diagenesis in lake sediments. Organic Geochemistry 20, 867–900.
Millar, C.I., Westfall, R.D., 2008. Rock glaciers and related periglacial landforms in the Sierra Nevada, CA, USA: inventory, distribution and climatic relationships. Quaternary International 188, 90–104.
Moser, K.A., Mordecai, J.S., Reynolds, R.L., Rosenbaum, J.G., Ketterer, M.E., 2010. Diatom changes in two Uinta mountain lakes, Utah, USA: responses to anthropogenic and natural atmospheric inputs. Hydrobiologia 648, 91–108.
Munroe, J., 2002. Timing of postglacial cirque reoccupation in the northern Uinta Mountains, northeastern Utah, USA. Arctic, Antarctic, and Alpine Research 34, 38–48.
Munroe, J., 2003. Holocene timberline and palaeoclimate of the northern Uinta Mountains, northeastern Utah, USA. The Holocene 13, 175–185.
Munroe, J.S., 2007. Properties of alpine soils associated with well-developed sorted polygons in the Uinta Mountains, Utah, USA. Arctic, Antarctic, and Alpine Research 39, 578–591.
Munroe, J.S., 2012. Lacustrine records of post-glacial environmental change from the Nulhegan Basin, Vermont, USA. Journal of Quaternary Science 27, 639–648.
Munroe, J. S. and Laabs, B. J. C., 2009. Glacial Geologic Map of the Uinta Mountains Area, Utah and Wyoming. Utah Geological Survey Miscellaneous, Publication 09–4DM, 1:100,000.
Munroe, J.S., Crocker, T.A., Giesche, A.M., Rahlson, L.E., Duran, L.T., Bigl, M.F., Laabs, B.J.C., 2012. A lacustrine-based Neoglacial record for Glacier National Park, Montana, USA. Quaternary Science Reviews 53, 39–54.
Nederbragt, A.J., Thurow, J., 2005. Geographic coherence of millennial-scale climate cycles during the Holocene. Palaeogeography, Palaeoclimatology, Palaeoecology 221, 313–324.
Nicholas, J.W., Butler, D.R., 1996. Application of relative-age dating techniques on rock glaciers of the La Sal Mountains, Utah: an interpretation of Holocene paleoclimates. Geografiska Annaler. Series A. Physical Geography 78A, 1–18.
Paasche, Ø., Dahl, S.O., Løvlie, R., Bakke, J., Nesje, A., 2007. Rockglacier activity during the Last Glacial–Interglacial transition and Holocene spring snowmelting. Quaternary Science Reviews 26, 793–807.
Refsnider, K.A., Brugger, K.A., 2007. Rock glaciers in central Colorado, USA, as indicators of Holocene climate change. Arctic, Antarctic, and Alpine Research 39, 127–136.
Reimer, P.J., Baillie, M.G.L., Bard, E., Bayliss, A., Beck, J.W., Blackwell, P.G., Ramsey, C.B., Buck, C.E., Burr, G.S., Edwards, R.L., Friedrich, M., Grootes, P.M., Guilderson, T.P., Hajdas, I., Heaton, T.J., Hogg, A.G., Hughen, K.A., Kaiser, K.F., Kromer, B., McCormac, F.G., Manning, S.W., Reimer, R.W., Richards, D.A., Southon, J.R., Talamo, S., Turney, C.S.M., van der Plicht, J., Weyhenmeyer, C.E., 2009. IntCal09 and Marine09 radiocarbon age calibration curves, 0–50,000 years cal BP. Radiocarbon 51, 1111–1150.
Reynolds, R.L., Mordecai, J.S., Rosenbaum, J.G., Ketterer, M.E., Walsh, M.K., Moser, K.A., 2010. Compositional changes in sediments of subalpine lakes, Uinta Mountains (Utah): evidence for the effects of human activity on atmospheric dust inputs. Journal of Paleolimnology 44, 161–175.
Rosenbaum, J.G., Reynolds, R.L., 2004. Record of late Pleistocene glaciation and deglaciation in the Southern Cascade Range. II. Flux of glacial flour in a sediment core from Upper Klamath Lake, Oregon. Journal of Paleolimnology 31, 235–252.
Rosenbaum, J.G., Reynolds, R.L., Colman, S.M., 2012. Fingerprinting of glacial silt in lake sediments yields continuous records of alpine glaciation (35–15 ka), western USA. Quaternary Research 78, 333–340.
Schaefer, J.M., Denton, G.H., Barrell, D.J.A., Ivy-Ochs, S., Kubik, P.W., Andersen, B.G., Phillips, F.M., Lowell, T.V., Schluechter, C., 2006. Near-synchronous interhemispheric termination of the last glacial maximum in mid-latitudes. Science 312, 1510–1513.
Schulz, M., Mudelsee, M., 2002. REDFIT; estimating red-noise spectra directly from unevenly spaced paleoclimatic time series. Computers & Geosciences 28, 421–426.
Sears, J., Graff, P., Holden, G., 1982. Tectonic evolution of lower Proterozoic rocks, Uinta Mountains, Utah and Colorado. Geological Society of America Bulletin 93, 990–997.
Shuman, B., 2003. Controls on loss-on-ignition variation in cores from two shallow lakes in the northeastern United States. Journal of Paleolimnology 30, 371–385.
Steinhilber, F., Beer, J., Fröhlich, C., 2009. Total solar irradiance during the Holocene. Geophysical Research Letters 36, L19704.
Strickland, J.D.H., Parsons, T.R., 1965. A manual of sea water analysis: with special reference to the more common micronutrients and to particulate organic material. Bulletin - Fisheries Research Board of Canada Fisheries Research Board of Canada Report 125, 203.
Stuiver, M., Reimer, P.J., 1993. Extended ^{14}C data base and revised CALIB 3.0 ^{14}C age calibration program. Radiocarbon 35, 215–230.
Wahrhaftig, C., Cox, A., 1959. Rock glaciers in the Alaska Range. Geological Society of America Bulletin 70, 383–436.
Wanner, H., Solomina, O., Grosjean, M., Ritz, S.P., Jetel, M., 2011. Structure and origin of Holocene cold events. Quaternary Science Reviews 30, 3109–3123.
Washburn, A., Goldthwait, R., 1958. Slushflows. Geological Society of America Bulletin 69, 1657–1658.
Williams, M.W., Baron, J.S., Caine, N., Sommerfeld, R., Sanford Jr., R., 1996. Nitrogen saturation in the Rocky Mountains. Environmental Science & Technology 30, 640–646.
Zielinski, G.A., 1989. Lacustrine sediment evidence opposing Holocene rock glacier activity in the Temple Lake Valley, Wind River Range, Wyoming, USA. Arctic and Alpine Research 22–33.